GMR
The Original

EFFECT OF MGO NANOPARTICLES ON THE MECHANICAL, THERMAL AND ELECTRICAL PROPERTIES OF LINEAR LOW-DENSITY POLYETHYLENE (LLDPE) NANOCOMPOSITES FOR CABLE APPLICATION

Bibhudatta Paikaray[1], Jayakrushna Moharana[2], Radhashyam Giri[3*]

[1]Department of Electrical Engineering, GITA Autonomous College, Bhubaneswar 752054, Odisha, India, affiliated with Biju Patnaik University of Technology, Rourkela, Odisha, Pin-769015
[2]Department of Electrical Engineering, HIT Bhubaneswar 752057, Odisha, India, affiliated with Biju Patnaik University of Technology, Rourkela, Odisha, Pin-769015
[3*]Department of Plastics Technology, CIPET: Institute of Petrochemicals Technology, Chennai 600032, Tamilnadu, India,
Email id: giripolymer@gmail.com

ABSTRACT
This study discusses with development of insulating materials for High Voltage Direct Current (HVDC) cable insulations by reinforcing nanomagnesia (MgO) particles with linear low-density polyethylene (LLDPE). The main work is to investigate the DC breakdown voltage performance of LLDPE/MgO nanocomposites as a function of filler. Increase in DC breakdown strength is very important for long-term reliability and safety of HVDC cable insulation. Besides electrical performance, tensile strength, thermal and morphological studies were made as complementary studies to check the mechanical, thermal stability and quality of particle dispersion. The LLDPE/MgO nanocomposites were prepared by melt blending technique with different ratios of MgO nanoparticles. A modifier was used to reduce the agglomeration of MgO nanoparticles inside the LLDPE matrix. DC breakdown voltage tests were conducted on the samples to determine their breakdown voltage. Improvements have been observed in tensile strength (23%), flexural strength (21.5%), impact strength (15.6%), thermal stability (35.42 °C), dielectric breakdown strength (48%) and melting point (3.4 °C) of 6 wt% MgO nanocomposites compare to neat LLDPE. Field Emission Scanning Electron Microscopy (FESEM) was undertaken to complement the results, which included the dispersion quality of MgO particles and the filler interfacial bonding. Results indicated that nanomagnesia incorporation improved the DC breakdown voltage of LLDPE, with the optimum value of 6 wt% MgO. At this loading, the material showed the strongest dielectric strength while retaining reasonable tensile properties. Thus, this study has proven that LLDPE reinforced with 6 wt% nanomagnesia is a viable and efficient insulation material for HVDC cable applications.

KEYWORDS: Antibacterial efficacy of sealants, Trypticase-yeast-cysteine-sucrose-bacitracin agar, mandibular first permanent molar

INTRODUCTION
The high-voltage industry is constantly evolving and modernizing power grid systems to provide reliable, cost-effective, and environmentally friendly energy solutions. Polyethylene is commonly used as an insulation material for HVDC cables due to its exceptionally high dielectric strength (approximately 800 MV/m), wide bandgap (8.8 eV), high resistivity, and availability in a uniform and ultra-clean form. Polyethylene is the most versatile polymers due to its low density, ease of processing, and affordability1-3. Linear low-density polyethylene (LLDPE) is a type of polyethylene with a density ranging from 0.915 to 0.940 g/cm³. It has a linear carbon chain with short, uniform branches that prevent the formation of ordered crystal structures. This characteristic gives LLDPE enhanced stiffness, strength, and ductility. LLDPE was also utilized for insulating wires and cables across low, medium, and high voltage applications 4-5. The primary distinction between LLDPE and LDPE lies in its narrow molecular weight distribution and lack of long-chain branching, which results in greater tensile strength and puncture resistance compared to LDPE. Being a saturated hydrocarbon similar to polyethylene, it is largely unreactive and resistant to alcohols, alkaline solutions, weak organic or inorganic acids, and saline solutions. Because of its excellent combination of flexibility and strength, LLDPE is widely used in various industrial applications, including packaging films; agricultural mulch, layflat pipes, water tubing, and low-temperature food containers, making it one of the most commonly used plastic materials worldwide 6-10. However, its use is limited by certain drawbacks, such as lower strength and poor heat resistance. To improve its properties, polyethylene nanocomposites containing various inorganic nanofillers have been developed in recent years 11-13. These nanocomposites offer significantly enhanced stiffness and tensile strength with only a slight increase in specific gravity compared to unmodified polyethylene. Nanofillers can be any material with at least one dimension (length, width, or thickness) ranging from approximately 1 to 30 nanometers. CuO, ZnO, SnO2, Al2O3, MgO, ZrO2 AgO, TiO2, CeO2, etc. are the examples of nanofillers as the size decreases in the nanoparticles; an increasing number of surface and interface

atoms generate strain or stress and adjoining structural perturbations 14-16. Wang and his colleagues conducted a study on nanocomposites based on LDPE and SiO2, examining their electrical resistivity and dielectric breakdown strength 17-18. Their findings indicated that incorporating SiO2 into the LDPE matrix enhanced properties. In another study, Juntao and his team investigated the impact of graphene oxide (GO) as a filler on the mechanical properties of LLDPE nanocomposites. The results showed that GO nanosheets significantly improved tensile strength, fatigue resistance, and hardness. Specifically, tensile strength, Young's modulus, and Shore D hardness increased by 27.4%, 31.3%, and 9%, respectively, with GO concentrations ranging from 0 wt.% to 2 wt.%. Additionally, GO had a notable effect on fatigue properties, leading to an almost exponential increase in cyclic durability. More study has gone into developing insulating materials based on polymers for use in high voltage cables. According to the aforementioned literature, several polymers such as polyethylene, cross-linked polyethylene, polydimethylsiloxane and polypropylene are utilized in cable applications. Fillers like MgO, Al2O3, ZnO, and TiO2 are utilized to improve the properties of base polymers 19-24. However, the literature review reveals that there is a dearth of work utilizing LLDPE as the basis polymer and MgO and TiO2 as property enhancers. Similarly, Amir Masoud Pourrahi and his collaborators explored the role of interfaces in polyethylene-metal oxide nanocomposites for ultra-high-voltage insulation. Their research indicated that using pure functionalized metal-oxide nanoparticles and highly porous micrometer-sized metal-oxide particles enhanced polyethylene's electrical insulation properties, as evidenced by charging current measurements over a defined period.
This study investigate the performance of LLDPE for HVDC applications by incorporating magnesim oxide nanoparticles in concentration of 1 phr to 8 phr and the properties for high voltage application is determined. This study examines the mechanical properties of the prepared nanocomposites, including tensile, flexural, impact strength to assess the influence of nanoparticles. Thermal stability and melt behaviour were evaluated using thermogravimetric analysis (TGA) and differential scanning calorimetry (DSC) respectively. The dielectric breakdown strength was also assessed to determine the composites suitability for high voltage cable applications. Obtained findings were compared based on filler characterestics and their loadings within in the LLDPE matrix

DETAILED MATERIALS AND METHODOLOGY

Materials

LLDPE was procured from Brahmaputra Cracker and Polymer Limited, Dibrugarh, Assam, PIN–786006, under the trade designation Brahma-Lene. LLDPE is synthesized through the copolymerization of ethylene with longer chain olefins. Its MFI is 7.0 g/10 mins at 190°C, and its density is 0.93 g/cm³ at 23°C. MgO nanoparticle was procured from adnano Technologies, Machenahalli Industrial Area, Shimoga-577222 Karnataka, with 99.0% purity, particle size < 100 nm, surface area 110-130 m2/g, density 1.07 g/cm3. Modifier C18 was obtained from Thermo Fisher Scientific India Pvt. Ltd, located at 402, Delphi 'B' Wing, Hiranandani Business Park, Powai, Mumbai – 400076. It has a purity of 90%, a boiling point of 170°C, a range of 13–17°C melting point, and 0.88 g/ml density. Irganox 1076 was acquired from N Shashikant and Co. (Mumbai, Maharashtra) with colorless and devoid of odour. The substance exhibited a pH value of 5.7, a melting point ranging from 50 to 550°C, thermal breakdown occurring above 350°C, a density of 1.02 g/cm³, and a molar mass of 530.87 g/mol. DCP was acquired from N Shashikant & CO. (Mumbai, Maharashtra). The predominant technique employed for high-voltage insulation is peroxide curing, with dicumyl peroxide being the preferred crosslinking agent.

Development of nanocomposites

The LLDPE/MgO (LM) nanocomposites were prepared using a Haake Rheomix OS internal mixer (Germany) with cam-type rotors, thereafter processed using a compression molding machine. The preparation of LLDPE/MgO nanocomposites was conducted through a melt compounding process with formulation shown in Table 1. The melt mixing process was conducted at 180°C with the speed of 40 rpm for 10 minutes duration. The prepared compound materials from sets were extracted following the mixing process and subsequently cooled using air. Subsequently, these were processed into uniform granules measuring 3×3 mm. The granules were subjected to drying in oven at 50°C for 30 minutes. Subsequent to the drying procedure, the granules were fed into the compression molding apparatus. Sheets of 140 mm × 140 mm × 3 mm (length, width, and thickness) with dimensions were produced at a temperature of 180°C utilizing a hydraulic press (George E. Moore Press, UK) for duration of 2 minutes under a pressure of 10 MPa. The mold was equilibrated to ambient temperature by flowing cold water through its platens under maintained pressure. The nanocomposite sheets were carefully removed from the mold and subsequently cut in to precise dimensions for additional testing and characterization.

Table 1. Sample description of LLDPE Nanocomposites

Polymer	Fillers	Modifier	Anti-Oxidant	Crossl inking Agent	Sample designation
LLDPE	MgO	C18a	Irganox 1076	DCP	
100	0.0	0.0	0.0	0.0	LL0
100	0.0	0.9	0.02	2.0	LM0
100	1.0	0.9	0.02	2.0	LM1
100	2.0	0.9	0.02	2.0	LM2
100	4.0	0.9	0.02	2.0	LM4
100	6.0	0.9	0.02	2.0	LM6
100	8.0	0.9	0.02	2.0	LM8

a Octadecyl (trimethoxy) silane (C18), Dicumyl Peroxide (DCP)

Experimental Details

Tensile strength Properties

The evaluation of tensile strength for the test specimens was conducted with the use of the Instron apparatus (model 5567, USA). The specimens, which were configured like dumbbells for the purpose of tensile testing, were fabricated per ASTM D-638 from nanocomposite sheets, utilizing a counter cutter machine 6490 (Ceast, Italy) along with calibrated templates. The samples conformed to the specified dimensions of 165 mm × 13 mm × 3 mm, while the apparatus operated at a velocity of 50 mm/min with a gauge length set at 50 mm.

Flexural strength Properties

Nanocomposite samples measuring 127 mm × 12.7 mm × 3 mm were evaluated for flexural strength utilizing JLW Instruments (Chicago, USA) in compliance with ASTM D-790. The samples were subjected for 48 hours at 23 ± 20C and 50 ± 5% relative humidity before testing

Impact strength Properties

The 'Impactometer 6545' device, manufactured by CEAST in Italy, was employed to perform the Izod impact test in accordance with ASTM D-256 with notch angle of 450 and a V-shaped notch that has a depth of 2.54 mm. The measurements for the specimen used to assess impact strength were 63.5 mm × 12.7 mm × 3 mm. The specimens were conditioned at 23 ± 10C and 55 ± 2% RH prior to testing.

Hardness

In accordance with ASTM D-2240, the Shore D durometer (Zwick Roell, Alexandria, USA) was used to measure the hardness of nanocomposites.

Field Emission Scanning Electron Microscopy (FESEM)

The surfaces of nanocomposite samples, which were etched, were examined using a Field Emission Scanning Electron Microscope (FESEM), specifically model No: JEOL JSM-5800 from Tokyo, Japan, to evaluate their phase morphology.

Electrical properties measurement

The measurement of DC volume resistivity was conducted with the Agilent 4339B, connected to the Agilent 16008B Resistivity Cell. A sample featuring a cross-sectional area of 10×10 cm^2 and a thickness of 0.2 cm was taken from the molded sheet and positioned between the electrodes of the resistivity cell, where it was subjected to a load of 5 kg. A reading was taken after 30 seconds of charging, and the resistivity was directly measured by applying 1 volt. With a frequency range of 10 to 106 Hz, the QuadTech 7600 LCR meter was used to measure the relative permittivity, dissipation factor, and AC resistivity. A specimen with 1 cm diameter and 0.1 cm thickness was employed for measurement purposes.

Dielectric Breakdown Strength (DBS)

The evaluation of dielectric breakdown strength (DBS) was performed utilizing the ASTM D-149 testing procedure with the Automatic Dielectric Breakdown Tester (Model-K16177, Koehler Instrument Company Inc., New York, USA). The ideal specimen type for this examination is a plaque that measures at least 4 inches in minimum dimension. The test sample is generated within a regulated laboratory setting, maintaining a relative humidity of 50 ± 5% and a temperature of 23 ± 2°C.

Thermogravimetric analysis (TGA)

Current study involves the use of TGA, Model No: Pyris 7–TGA & Make: Perkin Elmer, USA to evaluate the thermal behavior of the nanocomposite samples. The Samples ranging from 5 to 10 mg were positioned in an aluminum crucible and subjected to scanning from 30 to 800°C at a heating rate of 10°C/min within a nitrogen environment, maintaining a flow rate of 30 ml/min, while simultaneously documenting the associated weight loss.

Differential scanning calorimetry (DSC)

The DSC (Q100 V8.1 series, TA Instruments, USA) effectively evaluates glass transition temperature (Tg), melting temperature (Tm), crystallization temperature (Tc), and percentage crystallinity in polymer nanocomposite materials. The test was conducted using 5.0 ± 1.5 mg of sample for each batch throughout a temp range of 30 to +2000C for the nanocomposite samples at a scan rate of 100C/min in a liquid nitrogen atmosphere. The crystallinity percentage (% Xc) was determined using the formula $\%Xc = (\Delta Hc/\Delta H0) \times 100$. In this equation, ΔHc signifies the enthalpy heat of the nanocomposite samples, while $\Delta H0$ indicates the enthalpy heat for 100% crystalline LLDPE, which is set at 292 J/g.25

RESULTS AND DISCUSSION

Tensile strength Properties

The tensile characteristics, which encompass tensile strength, tensile modulus, and elongation at break, of LLDPE/MgO nanocomposites, are presented in Table 2. The data indicates that the tensile strength property of nanocomposite raises with higher nanofiller concentrations up to 6 phr in the LLDPE matrix, beyond which it decreases as filler concentration increases. LM6 nanocomposites to pristine LLDPE, the tensile strength increases by 23% at 6 phr loading of nanofillers. The observed rise in tensile strength can be linked to the reinforcing characteristics of nanofillers and their efficient distribution throughout the polymer matrix26-28.

Table 2. Tensile Properties of LLDPE/MgO Nanocomposites

Filler Concentration	Tensile strength (MPa)	Tensile modulus (MPa)	Elongation at break (%)
	LM	LM	LM
0	20.9 ± 1.6	580 ± 23	395 ± 34
1	21.2 ± 3.6	674 ± 35	378 ± 30
2	22.5 ± 5.2	679 ± 40	366 ± 24
4	23.9 ± 2.4	790 ± 51	354 ± 21
6	25.7 ± 3.5	815 ± 58	348 ± 19
8	22.7 ± 1.3	875 ± 61	332 ± 18

At elevated concentrations, agglomeration of nanoparticles in the polymer matrix may lead to a reduction in strength values after specific filler loading for LLDPE/MgO nanocomposites29. FESEM analysis allows for the observation of nanoparticle distribution within the polymer matrix. Fig. 1 (a-d) shows the FESEM micropraph of LM0, LM4, LM6 and LM8 nanocomposites, respectively. The FESEM micropraph shows that the nanoparticles are round in form. In FESEM Fig. 1 (b & c) for LM4 & LM6 nanocomposites, the nanoparticles are well distributed within the polymer matrix; whereas, in Figure 1 (d) for LM8 nanocomposites, the presences of some agglomeration within the polymer matrix, this is why; the strength of nanocomposites has reduced over their maximum loadings. Additionally, C18 silane modification contributes to better tensile strength, and increased resistance to moisture and environmental stress cracking, which are critical for long-term cable reliability. FESEM observations indicate relatively uniform filler dispersion up to 6 phr loading, with minimal agglomeration. This dispersion behavior directly corresponds to the observed improvement in mechanical properties, particularly tensile strength and elongation at break, which reach their maximum values at 6 phr. The enhanced properties at this loading are attributed to effective stress transfer arising from homogeneous filler distribution and improved interfacial interaction with the LLDPE matrix. At filler loadings beyond 6 phr, FESEM images reveal the onset of agglomeration, which coincides with a reduction in mechanical performance. Such agglomerates act as stress-concentration sites, leading to premature failure and diminished reinforcement efficiency. Table 2 indicates that the tensile modulus of LLDPE/MgO nanocomposites has enhanced with the maximum concentration of nanofillers. The tensile modulus of pristine LLDPE is 580 MPa. In contrast, the modulus values for 8 phr loaded LLDPE/MgO nanocomposites are 875 MPa respectively. Consequently, the modulus values for 8 phr loaded LLDPE/MgO nanocomposites exhibit increments of 50.8% respectively, in comparison to neat LLDPE. The ongoing increase in modulus value up to the highest filler concentration indicates that the fillers function as a reinforcing agent at low strain levels.

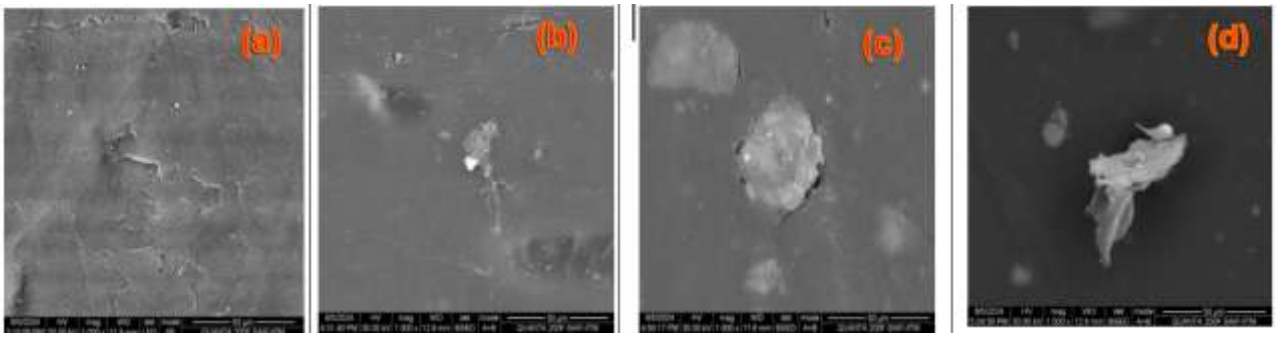

Figure 1. FESEM micrographs of (a) LM0, (b) LM4, (c) LM6 and (d) LM8 nanocomposites

The data shows a progressive decrease in the elongation at break results for nanocomposites sets as the nanofiller loading reaches its maximum level. Incorporation of nanofillers into the polymer matrix may restrict the mobility of polymer chains, leading to a reduction in the elongation at break results. The elongation at break results for neat LLDPE and LM8 nano composite are 395% and 332% respectively. This demonstrates a decrease of 15.9% in elongation at break results for LM8 nanocomposites, respectively, when compared to neat LLDPE.

Flexural Strength properties

The flexural properties, which encompass flexural strength and flexural modulus, relate to the bending forces applied to a material until a defined deflection or breakage takes place in the specimen. Table 3 displays the values of flexural strength and modulus for the examined samples of LLDPE/MgO nanocomposites.

Table 3. Flexural properties of LLDPE/MgO Nanocomposites

Filler Concentration	Flexural strength (MPa)	Flexural modulus (MPa)
	LM	LM
0	23.2 ± 2.7	352 ± 46

1	25.6 ± 3.4	367 ± 48
2	26.5 ± 3.6	412 ± 52
4	27.7 ± 3.7	434 ± 58
6	28.2 ± 3.9	562 ± 65
8	27.2 ± 3.4	586 ± 74

Table 3 indicates that the flexural strength values of nanocomposites LLDPE/MgO increase with the concentration of nanofillers up to 6 phr within the LLDPE matrix, followed by a decline with further increases in filler concentration. The flexural strength of LM6 nanocomposites increased by 21.5% respectively, at a loading of 6 phr nanofillers compared to neat LLDPE. The pristine polymer LLDPE is non polar in nature. Conversely, the nano fillers, MgO exhibit polar characteristics. There will be a reduced interaction and reinforcement between the pristine polymer and nano filler particles. As a result, a rise in strength has been noted during the preliminary concentration phase. The decrease in strength observed under conditions of high concentration can be ascribed to the clustering of particles within the polymer matrix. The flexural modulus of LLDPE/MgO nanocomposites consistently increases with higher filler particle loadings. The modulus value of 8 phr loaded LLDPE/MgO nanocomposites increased by 66.1% respectively.

Impact Strength and hardness properties

Impact strength refers to the amount of energy a material can withstand before breaking when subjected to a sudden force. Table 4 presents the results of the Izod impact test conducted on the LLDPE/MgO nanocomposites.

Table 4. Impact strength and hardness of LLDPE/MgO nanocomposites

Filler Concentration	**Impact strength (J/m)**	**Hardness (shore D)**
	LM	LM
0	38.4 ± 4.8	43.2 ± 4.5
1	39.6 ± 5.1	44.5 ± 4.8
2	40.5 ± 5.5	45.7 ± 5.1
4	42.4 ± 5.8	46.8 ± 5.4
6	44.4 ± 5.2	47.5 ± 5.8
8	41.2 ± 5.6	48.4 ± 6.1

The impact strength of LLDPE/MgO nanocomposites increases with up to 6 phr filler loading, followed by a decline at 8 phr loading. The impact strength values for neat LLDPE, 6 phr loaded LLDPE/MgO nanocomposite are 38.4 and 44.4 J/m, respectively. Consequently, improvements in strength of 15.6% are noted for 6 phr loaded LLDPE/MgO nanocomposites, respectively, in comparison to the base LLDPE. The improvement in impact strength is ascribed to the efficient interfacial bonding between the polymer matrix and the nano filler particles. The decline in performance of the highest loaded nanocomposites may result from nonhomogeneous particle distribution and agglomeration, which facilitate crack propagation and lead to sample failure. Table 4 presents the Shore D hardness values for LLDPE/MgO nanocomposites. The hardness value of the nanocomposites has shown a consistent increase with the addition of MgO. The increase in hardness value for 8 phr loaded LLDPE/MgO nanocomposites is 12.03% respectively, in comparison to pristine LLDPE. The density and hardness values of MgO exceed those of pristine LLDPE. Consequently, the nanocomposites demonstrate a high hardness value.

Electrical resistivity

Figures 2 (a) illustrate the electrical DC resistivity, while Figures 2 (b) depicts the AC resistivity of LLDPE/MgO nanocomposite sets, respectively. The DC resistivity is presented in relation to MgO filler loadings, while the AC resistivity is discussed w.r.t frequency of electric field. Figure 2 (a) demonstrates that the direct current resistivity of nanocomposite samples diminishes with the addition of nano fillers into the polymer matrix. The decrease in electrical resistivity depends on the energy associated with the band gap. The mobility of electrons and charge carriers in composite systems is improved by the addition of nanofiller particles to the polymer matrix, which lowers the band gap energy. The incorporation of nano filler particles into the polymer matrix reduces the band gap energy, thereby enhancing the mobility of electrons and charge carriers in the composite systems30.

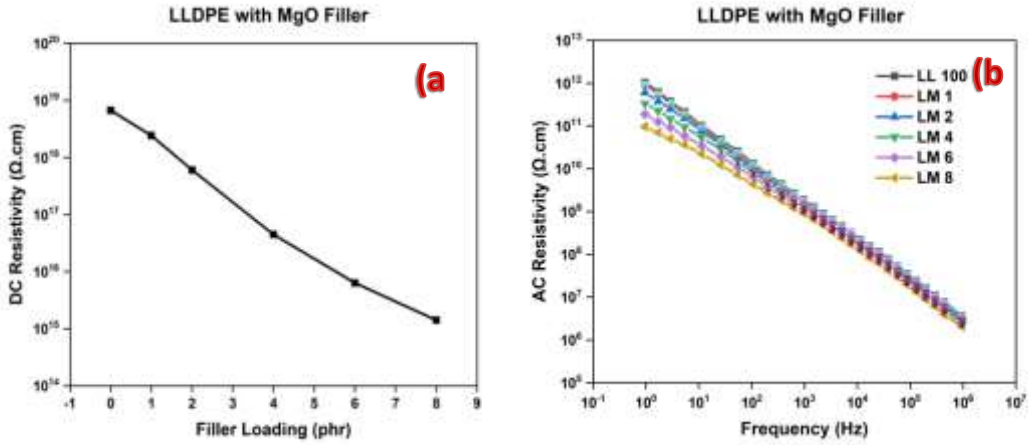

Figure 2. (a) DC resistivity of MgO nanocomposites, (b) AC resistivity of MgO nanocomposites

The incorporation of the nano fillers results in a reduction of electrical resistivity. In polymer composite systems, electrical conduction is governed by multiple factors, including filler dispersion, interfacial polarization, and formation of conductive pathways, charge carrier hopping/tunneling and microstructural changes within the polymer matrix. The reduction in resistivity arises from a combination of improved filler dispersion and interfacial interaction up to 6 phr loading, which facilitates charge carrier transport through hopping and tunneling mechanisms, rather than a direct band gap narrowing alone. The electrical resistivity of LM8 nanocomposites exhibits reductions of approximately 104 orders, respectively, when compared to pristine LLDPE. The plots of AC resistivity versus electric field frequency Figure 2 (b) indicate that the base polymers and the composites from sets exhibit frequency-dependent characteristics. Resistivity decreases as frequency increases. The trends of decrement observed in LLDPE/MgO composites exhibit a linear pattern. The resistivity observed in this area is ascribed to the contributions from direct current (DC) and alternating current (AC). Similar to direct current (DC) resistivity, the alternating current (AC) resistivity exhibited a decrease with incorporation of nano filler loading in the LLDPE polymer matrix. This can be elucidated in a manner analogous to what was previously outlined for DC resistivity.

Dielectric constant and dielectric loss

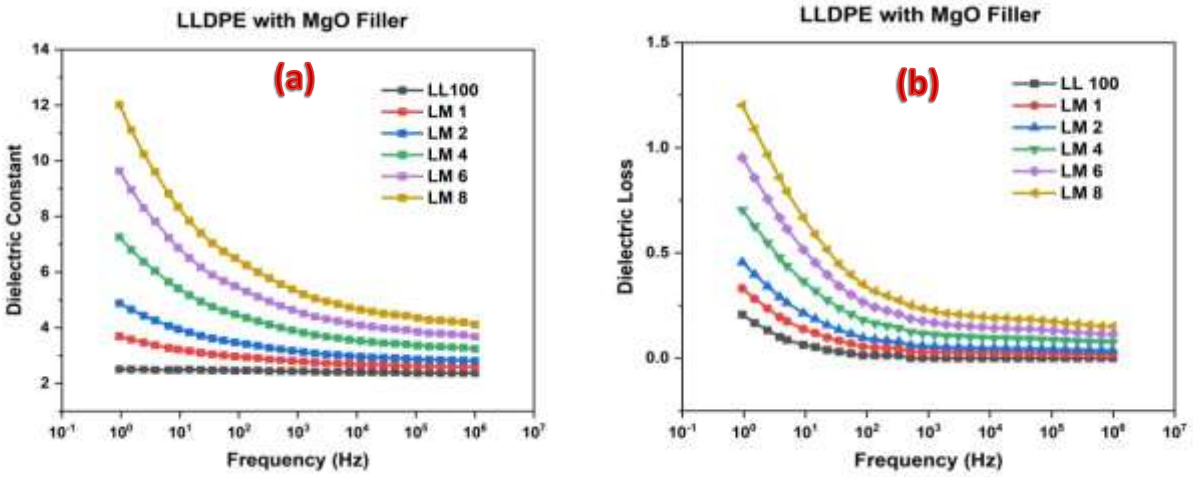

Figure 3. (a) Dielectric constant of MgO nanocomposites and (b) dielectric loss of MgO nanocomposites

Dielectric loss is the dissipation of charge from a substance, whereas the dielectric constant represents the material's ability to store charge. The loss and dielectric constant results of MgO incorporated LLDPE/MgO nanocomposite samples are presented in Figure 4, with respect to frequency at varying filler loadings. Figures 3 (a) present the dielectric constant plots, while Figures 3 (b) illustrates the dielectric loss plots for LLDPE/MgO nanocomposites. The graph indicates that the ability to store charge value of the pristine polymer and low concentration nanocomposites is independent of frequency. Nanocomposites with high filler loading demonstrate frequency-dependent behavior. The capacity of a material to retain charge is derived from the polarization that develops within it when subjected to an external electric field. Polarizations are classified into four distinct types: atomic, molecular, interface, and electrode 29, 31. The embedded nano filler particles within the polymer matrix operate as a nano capacitor. In pristine LLDPE and low-filled nanocomposites, the polarization is defined by atomic and molecular characteristics, leading to a diminished dipole orientation when subjected to an electric field. The dielectric constant exhibits near frequency independence. The incorporation of larger quantities of fillers leads to a greater polarization at the interface between the fillers and the polymer, suggesting an increase in the number of capacitors. This phenomenon explains the behavior of nanocomposites that is dependent on frequency, as well as the noted rise in the dielectric constant in relation to the amount of filler used.

At a frequency of 1 kHz, the material's ability to store charge values for pristine LLDPE and LM6 nanocomposite are 2.3 and 10.8 respectively. Consequently, the dielectric constant values for LM6 nanocomposites exhibit increases of 370% respectively, in comparison to neat LLDPE. Figure 3 (b) illustrate the variations of dissipation of charge as a function of frequency for LLDPE/MgO nanocomposite systems, respectively. The loss values at lower frequencies regions are higher than those at higher frequency regions. The considerable loss of charge in the lower frequency range can be ascribed to the strong alignment of dipoles. Energy is essential for the alignment of dipoles with the electric field. At lower frequencies, dipoles are afforded more time to align with the electric field. Consequently, proper orientation is achieved, leading to an increase in loss. The graph indicates that the dissipation of charge value rises as the fillers loading increases. As the concentration of filler rises, there is a corresponding increase in the quantity of nano capacitors.

The low-frequency enhancement in dielectric permittivity is attributed to interfacial polarization arising from charge accumulation at polymer–filler interfaces, whereas the relaxation observed at intermediate frequencies is governed by dipolar polarization associated with molecular dipole reorientation. The sharp increase in permittivity at very low frequencies is assigned to electrode polarization, which is an extrinsic measurement effect rather than an intrinsic bulk property. The dispersed high-permittivity nanofillers introduce numerous interfaces within the polymer matrix. Under an applied field, these interfaces lead to enhanced charge storage and localized polarization effects often discussed in the literature as 'nano-capacitor' behavior, where each filler/matrix interface acts analogously to a capacitive element, contributing to an increased effective dielectric constant and tailored dielectric response32-33. Consequently, additional energy is dissipated due to their alignment with the electric field. The dissipation of charge value increases as a result. At high filler loadings, the frequency-dependent dielectric response of polymer nanocomposites is governed primarily by charge transport phenomena, filler-induced heterogeneity, and dipolar relaxation constraints, rather than interfacial polarization. As filler concentration increases, the polymer matrix continuity is progressively disrupted, altering local electric field distribution and charge dynamics. At low frequencies, the increase in dielectric loss (tan δ) observed at higher filler contents can be attributed to enhanced charge carrier mobility and accumulation within the amorphous regions of the polymer, facilitated by the presence of filler surfaces and defect sites. High filler loading increases the probability of localized charge trapping and de-trapping, hopping conduction between adjacent filler particles due to reduced inter-particle distance. At higher frequencies, dipolar entities within the polymer matrix and at polymer–filler interfaces are increasingly unable to orient in phase with the applied field. While this results in a reduction in dielectric permittivity (ε′), dielectric loss does not decrease proportionally at high filler loadings. For cable insulation materials, dielectric loss must be minimized across operational frequency ranges to prevent thermal build-up, insulation degradation, and premature electrical ageing. The results clearly indicate that excessive filler loading is detrimental, as loss mechanisms driven by conduction and relaxation constraints dominate over any permittivity enhancement.

Dielectric Breakdown Strength (DBS)

The maximum electrical potential known as dielectric breakdown strength (DBS) value for LLDPE/MgO nanocomposites have been compared to the behavior of pristine LLDPE, as illustrated in Figure 4

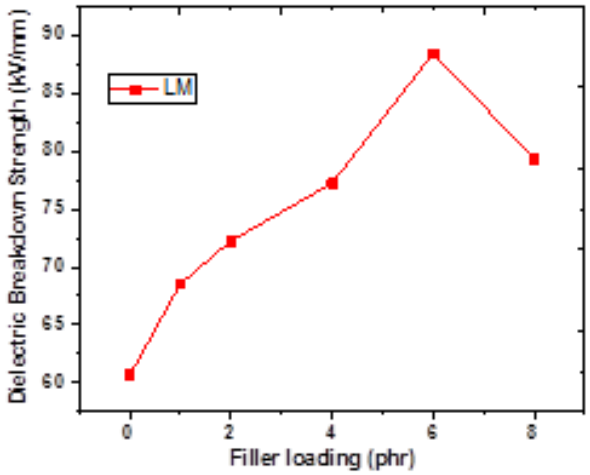

Figure 4. DBS of LM nanocomposites sample with various nano fillers concentration

Figure 4 illustrates that the addition of 6 phr of MgO nanofillers into the LLDPE matrix leads to an enhancement in the maximum electrical potential strength values for categories of nanocomposite samples, achieving levels of 89 kV/mm respectively. The incorporation of 6 phr of MgO into the polymer matrix yielded the maximum electrical potential strength relative to other sample. The increments are 48% for 6 phr filled MgO nanocomposites, respectively. The incorporation of MgO at loadings exceeding 6 phr has significantly reduced the electrical potential strength of the LLDPE/MgO nanocomposites. The increase in electrical potential strength of LLDPE, achieved through the incorporation of up to 6 phr of nanofillers, can be ascribed to the barrier effect that these nanofillers provide. LLDPE is inherently non-polar, which leads to poor interfacial compatibility with polar inorganic nanofillers such as metal oxides. C18 silane modifiers address this limitation through effective surface modification. C18 alkyl chain provides excellent hydrophobicity and strong

affinity toward the LLDPE matrix, while the silane functional group chemically bonds with hydroxyl groups present on the nanofiller surface. This dual functionality significantly improves filler dispersion, reduces agglomeration, and strengthens interfacial adhesion between the polymer and the nanofiller. For cable application, the improved interfacial interaction translates into enhanced electrical insulation properties, including higher dielectric strength and reduced space-charge accumulation. The addition of nanofillers in LLDPE/MgO nanocomposites may prolong tree propagation time, while accelerated test results indicate an enhancement in dielectric breakdown strength. Exceeding, a filler concentration of 6 phr leads to defects at the interfaces, along with an increase in voids and cracks, which deteriorates the electrical potential strength properties. The breakdown strength of 8 phr loaded MgO filled LLDPE nanocomposites have decreased. The agglomeration of MgO nanoparticles (Figure 1) results in clusters that act as electrical defects.

Thermogravimetric Analysis (TGA)

Thermogravimetric Analysis (TGA) has been employed to assess the thermal stability of neat LLDPE and LLDPE/MgO nanocomposites. Figure 5 (a) illustrates the TGA plots, highlighting extracted parameters including the onset of degradation temperature (Tonset), the maximum degradation temperature (Tmax), and the percentage residue, which are summarized in Table 5.

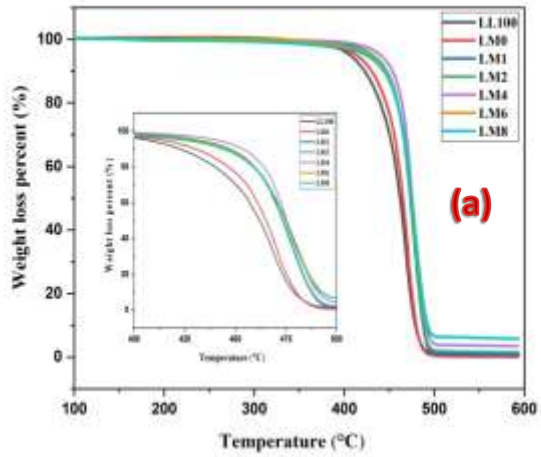

Figure 5. (a) Thermogravitograms of LM nanocomposites

Degradation onset occurs at 95% weight loss, with a % residue observed at 600°C. The figure demonstrates that pristine LLDPE and its nanocomposites filled with MgO undergo degradation in a single stage. The degradation onset for pristine LLDPE occurs at 413.21°C, which is elevated for LM nanocomposites. The incorporation of MgO has resulted in increased onset degradation relative to neat LLDPE. The temperature at which degradation begins has risen more significantly for composites containing 6 phr in comparison to those with 8 phr. The rise in onset degradation temperature is recorded at 35.42°C for LM6 nanocomposites, when compared to the neat LLDPE. Pristine LLDPE exhibited a maximum degradation temperature (Tmax) of 484.21°C. The incorporation of MgO has significantly elevated the T max value across all examined nanocomposite samples. The maximum degradation temperatures for LM (506.29 °C) nanocomposites are observed at a loading of 6 phr. The increases in maximum degradation are 22.08 °C for the respective LM6 nanocomposites. Linear low-density polyethylene (LLDPE) exhibits poor thermal conductivity. As a result, when thermal energy is introduced, the polymer chains start to break down once the thermal energy exceeds the bond energy of the polymer. Consequently, polymer degradation occurs at relatively lower temperatures. Unlike LLDPE and MgO exhibit thermal conductivity. Furthermore, there are interactions between polymer matrices and nano filler particles. These two elements improve the composites' capacity to withstand thermal energy by dispersing it, thus averting localization. A greater amount of heat energy is necessary for the decomposition of a material when there is increased interaction among the materials in the system. The composites demonstrate enhanced thermal stability. The residue percentage at 600°C for neat LLDPE is 0.58. The value has been progressively elevated following the incorporation of nanofillers into the polymer matrix. The noted gradual rise in the percentage of residue can be ascribed to the incorporation of greater amounts of fillers that remain stable at this temperature. Additionally, C18 silane modification contributes to better thermal stability for long-term cable reliability.

Table 5. TGA Data of neat LLDPE and LLDPE/MgO nanocomposites

Filler Concentration	Tonset (0C)	Tmax (0C)	% Residue at 6000C
	LM	LM	LM
0	413.21	484.21	0.58
1	440.48	499.83	1.21
2	443.33	501.18	2.01
4	448.23	506.02	5.84

6	448.63	506.29	6.36
8	441.92	503.66	6.37

Differential scanning calorimetry (DSC)

The melt temperature and percentage crystallinity of pristine LLDPE and LM nanocomposites were examined using differential scanning calorimetry (DSC), with the corresponding plots displayed in Figure 6 (a). The parameters extracted from the graph are presented in Table 6. The extracted values include melting temperature and crystallization temperature. The table indicates that the melting point of neat LLDPE is 120.83 °C. The incorporation of nanoparticles into the polymer matrix has resulted in an elevated melting point temperature.

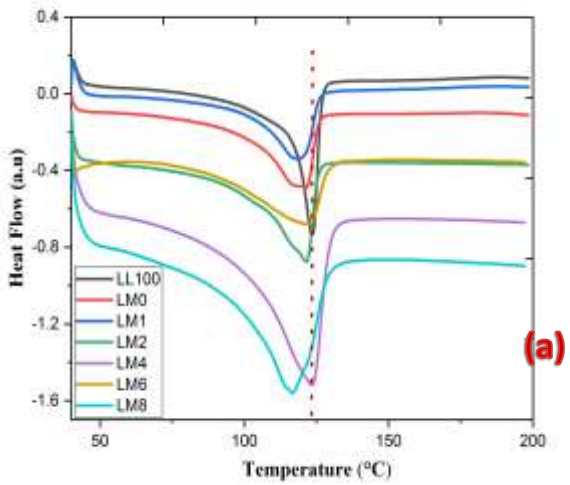

Figure 6. (a) DSC thermograms of LM nanocomposites

The most significant rise in the initiation of melting and the temperatures at which melting occurs is noted in 6 phr concentrations of LM nanocomposites. The data indicates an increase in melting peak temperature of 6.06°C for LM6 nanocomposites. The noted enhancement in melting characteristics can be ascribed to the interplay between the polymer and the filler, in addition to the elevated specific heat capacity of the nanofillers.34-35

Table 6. Melting temperature (Tm) and crystallinity (%Xc) of LLDPE/MgO nanocomposites

Filler loading	LM	
	Tm (0C)	%Xc
0	120.83	52.61
1	121.27	49.54
2	122.16	48.64
4	126.24	47.55
6	126.89	46.64
8	121.74	45.74

The incorporation of fillers exceeding 6 phr loading has demonstrated a detrimental effect, resulting in decreased melting peak temperatures for LM8 nanocomposites. This decrease may result from inadequate dispersion of nanofiller particles within the polymer matrix. The percentage of crystallinity has progressively decreased following the incorporation of MgO nanofillers. The percentage of Xc for pristine LLDPE is 52.61%. The reduction is 45.74% for LM8 nanocomposites. The reduced crystallinity of polymer composites can be attributed to the addition of nanofillers, which create obstacles in e proper orientation of molecular chains during cooling.

CONCLUSIONS

Effectively prepared LLDPE/MgO nanocomposites and characterized their various properties. The Mechanical properties (tensile strength, flexural strength, impact strength) and dielectric breakdown strength of nanocomposites exhibited an increase up to a specific filler loading, after which a decline was observed. The Mechanical properties (tensile strength, flexural strength, impact strength) and dielectric breakdown strength demonstrate increases of 23%, 21.5%, 15.6%, 4.5%, 48%, and 41% respectively, when 6 phr loaded LM nanocomposites are utilized. The elongation at break has diminished since the commencement of filler loading. The enhancement in strength is attributed to efficient interactions between the polymer and filler at minimal filler loadings. Increased loading leads to filler agglomeration, which results in a decline in properties. The nanocomposites exhibit enhanced electrical conductivity, permittivity, thermal stability, and melting point when compared to neat LLDPE. The addition of fillers has resulted in a reduction of crystallinity. The obstruction created by filler particles may lead to difficulties in the correct alignment of polymer chains throughout the crystallization process. The results indicate that nanocomposites are suitable for high voltage cable applications

REFERENCES

1. Z. Li, K. Okamoto, Y. Ohki, T. Tanaka, in Proceedings of the IEEE 9th International Conference on the Properties and Applications of Dielectric Materials, ICPADM 2009 – Harbin, China, 2009, 753.
2. K. Shah, R. Jain, V. Shrinet, A. Singh, D. Bharambe, IEEE Trans. Dielectr. Electr. Insul. 2009, 16, 853.
3. W. Wang, S. Li, F. Tang, J. Li, IEEE Annual Report Conference on Electrical Insulation and Dielectric Phenomena, Montreal, Canada 2012, 521.
4. R. Ramkumar, C. P. Sugumaran, IEEE 7th Power India International Conference (PIICON), Bikaner, India 2016, 1.
5. X. Chen, L. Yu, C. Dai, A. Paramane, H. Liu, Z. Wei, Y. Tanaka, IEEE Trans. Dielectr. Electr. Insul. 2019, 26, 2041.
6. X. Chen, A. Paramane, H. Liu, J. Tie, Z. Wei, Y. Tanaka, Polym. Eng. Sci. 2020, 60, 717.
7. M. Saleh, Z. Al-Hajri, A. Popelka, S. Javaid Zaidi, Materials 2020, 13, 250.
8. Diaa-Eldin A. Mansour, Nagat M. K. Abdel-Gawad, Adel Z. El Dein, Hanaa M. Ahmed Mohamed M. F. Darwish, and Matti Lehtonen Materials 2021,14.16.
9. Pollyana Melo Cardosa , Marcelo Massayoshi Ueki , Josiane Dantas Viana Barbosa, Williams Teles Barbosa, Benjamine Lazarus and Joyce Batista Azevedo Polymers 2022,14.3723
10. Ilona Plesa , Petru V Notingher , Cristina Stancu , Frank Wiesbrock and Sandra Schlogl Polymers 2019,11,24.
11. Jaroslav Hornak , Jiri Kopriva , Zdenek Jansa , Pavel Prosr, Anton Baran , Pavel Trnka Surface and inerfaces 46(2024)104112.
12. B. Nageshwar Rao, S . Vynatheya, R. Kandiban ICD.2018.8470039.
13. G.F Movikov , E.V. Rebenok , K.A.Kydralieva , and G.I. Dzhardimalieva ISSN 0036- 0244,Russian journalof Physical Chemistry a vol.93, No 12,pp.2424-2428.
14. Jianying Li, Kai Yang, Kangning Wu, Zhenghong Jing , Jin – Yong Dong 2023 ;IET Nanodielectr;6:130 -146.
15. Burjupati Nageshwar Rao , Nandakumar V.S Materials today: proceedings18(2019)994 – 1005.
16. E.Kontou , M .Niaounakis (2006) Polymer 47(2006) 1267-1280.
17. Amiir Masoud Pourrrahimi,Richard T .Olsson,and Mikael S .Headenqvist (2018) Advanced materials.2018,30.1703624.
18. Ranjeetkumar Gupta, Lindsay Smith, James Njuguna, Alan Deighton, and Ketan Pancholi ACS Applied Electronic Materials, 2020.
19. Abdelrahman Said, Amira Gamal Nawar, Elsayed Alaa Eldesoky, Samir Kamel, and Mousa Awdallah Abd-Allah .American Journal of Polymer Science and Technology, 2020.
20. Yang, L., Wu, K., & Peng, H. (2020). IEEE Transactions on Dielectrics and Electrical Insulation, 27(3), 1235-1246.
21. Kashi, S., Varley, R., & Simon, G. (2018) Journal of Applied Polymer Science, 135(24), 4567.
22. Tanaka, T., Montanari, G. C., & Mülhaupt, R. (2004). IEEE Transactions on Dielectrics and Electrical Insulation, 11(5), 763-784.
23. Zhang, J., Gao, F., & Liu, Y. (2019) Materials Science and Engineering: B, 246, 114-122.
24. Chen, Y., Wang, J., & Xu, X. (2022) Materials Today Communications, 30, 103045.
25. Cardoso P M, Ueki M M, Barbosa J D V, Barbosa W T, Lazarus B, Azevedo J B. Development and Characterization of LLDPE Blends with Different UHMWPE Concentrations Obtained by Hot Pressing. Polymers 2022; 14: 3723, 1-12.
26. Islam M, Rahaman M, Aldalbahi A, Paikaray B, Moharana J, Mondal S, Das N C, Gupta P, Giri R. High density polyethylene and metal oxides based nanocomposites for high voltage cable application. J. Appl. Polym. Sci. 2022; 139 (11): 51787, 1-15.
27. Manna R, Nayak S, Rahaman M, Khastgir D. Effect of annealed titania on dielectric and mechanical properties of ethylene propylene diene monomer-titania nanocomposites. e-Polymers. 2014; 14(4): 267–275.
28. Sohail O B, Bin-Dahman O A, Rahaman M, Al-Harthi M A. Effect of aluminum nitride concentration on different physical properties of low density polyethylene based nanocomposites. Journal of Polymer Engineering. 2017; 37 (8): 765–775.
29. Li Z.; Du B. Polymeric Insulation for High-Voltage DC Extruded Cables: Challenges and Development Directions. IEEE Electr. Insul. Mag. 2018; 34(6):30–43.
30. Bin-Dahman O A, Rahaman M, Khastgir D, Al-Harthi M A. Electrical and Dielectric Properties of Poly(Vinyl Alcohol)/Starch/ Graphene Nanocomposites. Can. J. Chem. Eng. 2018; 96(4), 903-911.
31. Liao C Z, Tjong S C. Mechanical and Thermal Performance of High-Density Polyethylene/Alumina Nanocomposites. J. Macromol. Sci. Part B. 2013; 52 (6): 812-825.
32. Wang S, Luo Z, Liang J, Hu J, Jiang N, He J, Li Q. Polymer Nanocomposite Dielectrics: Understanding the Matrix/Particle Interface. ACS Nano. 2022: 16 (9): 13612–13656
33. Hornak J, Trnka P, Kadlec P, Michal O, Mentlík V, Šutta P, Csányi G M, Tamus Z Á. Magnesium Oxide Nanoparticles: Dielectric Properties, Surface Functionalization and Improvement of Epoxy-Based Composites Insulating Properties. Nanomaterials. 2018; 8:381. doi:10.3390/nano8060381
34. Mohamed E M, Mohammed A K, Mahues R. Y, Rehab M. El-S. Influence of MgO and ZnO as nano-additives on the mechanical, microstructural and thermal performance of high-density polyethylene. J Appl Polym Sci. 2022; 139:1-17.
35. Hamzah M S, Jaafar M, Mohd Jamil M K. Electrical insulation characteristics of alumina, titania, and organoclay nanoparticles filled PP/EPDM nanocomposites. J. Appl. Polym. Sci. 2014; 131(23): 41184. 10.1002/app.41184.